MADRID
inter.noise 2019
June 16 - 19
NOISE CONTROL FOR A BETTER ENVIRONMENT

Development and validation of a computational methodology for the calculation of fluid-structure-acoustic interactions on a simplified car model

Seidler, Marcel[1]
Friedrich-Alexander-University Erlangen-Nürnberg
Cauerstraße 4
91058 Erlangen, Germany

Nusser, Katrin
Friedrich-Alexander-University Erlangen-Nürnberg
Cauerstraße 4
91058 Erlangen, Germany

Becker, Stefan
Friedrich-Alexander-University Erlangen-Nürnberg
Cauerstraße 4
91058 Erlangen, Germany

ABSTRACT

In the sound spectrum of passenger cars, the turbulence development behind the side mirror is a highly significant process, as the interactions of the turbulent structures with the side window lead to vibration and thus to sound radiation into the vehicle interior. Therefore, the understanding of the coupling of exterior flow, structural vibration and sound propagation is crucial for a simulative reproduction and the realistic prediction of the perceptible sound spectrum inside the vehicle.

While previous investigations focused mainly on isolated aspects of the described test case, this study aims at the introduction of a complete simulative methodology, which also includes the window clamping elasticity and the acoustic properties of the vehicle interior. The main challenge lies in the implementation of the coupling strategy, as the accuracy of the fluid-structure-acoustic interaction at the side window is essential for the result quality. Considering different coupling approaches a one-way data transfer between flow and structure is chosen, while the acoustic propagation is fully coupled to the window vibration through a calculation in the frequency domain. The simulation results are in good accordance with wind tunnel measurements, but also show local deviations, which are subject to a final discussion.

Keywords: Vehicle Sound, Mirror, Fluid-Structure-Acoustic Interaction
I-INCE Classification of Subject Number: 76

[1] se@ipat.fau.de

1. INTRODUCTION

Through the trend to electromobility a rapid change in automotive sound design is developing. The focus of acoustic car design increasingly moves towards aeroacoustic processes and their user orientated optimization. In the wide range of possible sources involved, the flow around and turbulence production behind the mirror geometry is one of the most shaping processes, as the side window, which is directly influenced by the induced turbulent structures, embodies a direct interface between exterior excitation and passenger's perception.

The induced turbulent structures in front of the side-window lead to unsteady pressure fluctuations on the window surface and thus to vibration and radiation of acoustic sound into the vehicle interior.

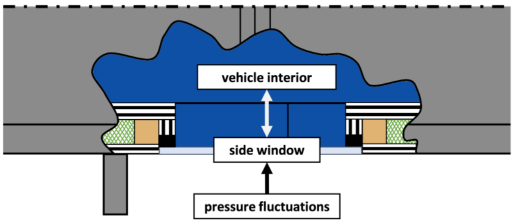

Figure 1: Schematic visualization of the test case

The reproduction and prediction of the thereby produced sound spectrum in the vehicle interior has been subject to a wide range of research. But seldomly, current research includes the whole range of contributing factors, but merely discusses individual mechanisms. Based on results from current research this paper introduces a fluid-structure-acoustic interaction simulation strategy, which allows the systematic analysis of side-mirror induced noise in the driver's cabin. Additionally, the value and flexibility of the methodology is tested within the investigation of individual involved mechanisms. This research paper thereby continues the work of Müller [1], who researched the described test case, focusing on a metrological approach.

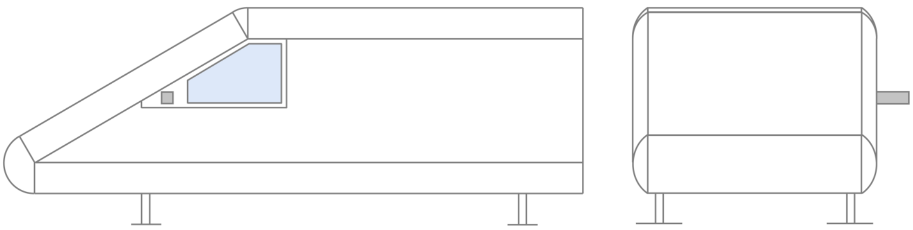

Figure 2: Geometry of the SAE body, used in the research of Müller [1]

To benefit from the measurements performed by Müller the same SAE body, with similar boundary conditions is chosen for the conduction of the simulative approach.

2. NUMERICAL SETUP

For the numerical approach two different simulations inside the Ansys software environment are performed: The fluid simulation for the flow around the SAE body and a coupled vibro-acoustic analysis for the calculation of the perceptible sound spectrum inside the vehicle.

2.1. Implementation of the flow simulation

Beginning with the exterior flow, a CFD simulation is performed with Fluent V17.1. For the CFD scheme, the hybrid DES (Detached Eddy Simulation) approach is extended by the delayed option, which provides a more effective protection of the RANS boundary layer near the window. As turbulence model the k-ω-SST formulation with a second order discretization in time and space is chosen (except for momentum, which is BCD by default). The simulation time step is set to $\Delta t = 3 \cdot 10^{-5} s$.

The geometrical set up in the CFD approach consists of the SAE body shown in figure 2, which is placed in a generic wind tunnel (see fig. 3). Through local mesh refinements near the mirror, the spatial mesh resolution on the window surface is reduced to 1 *mm*, which simultaneously defines the interface resolution for the fluid-structure coupling.

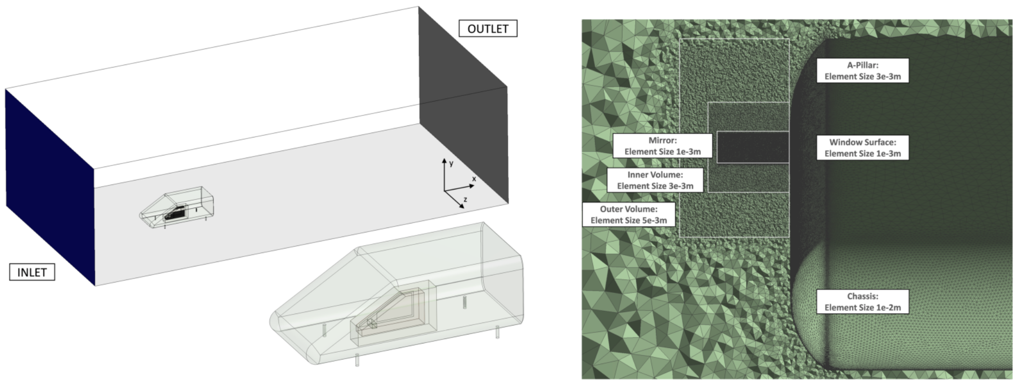

Figure 3: Computational domain and mesh configuration

Under the condition that all convergence criteria are met, the flow induced pressure distribution on the window surface is exported for every time step and later transformed into the frequency domain. The frequency transformed data is then exported in the *cgns.* file format and thereby transferred to the vibroacoustic simulation set up.

2.2. Implementation of the vibroacoustic simulation

The mechanical simulation of the window is directly coupled to the interior acoustic simulation via the Acoustics Extension provided by Ansys. Therefore, the acoustic simulation model consists of the SAE body interior and the side window.

Through the combined modelling and meshing of window and acoustic body, a conformal interface is produced for the coupling of structural vibration and acoustic propagation. To avoid interpolation errors during the mapping of the *cgns.* data, a 3 *mm* shell mesh is chosen for the window, while the main acoustic body is meshed with 15 *mm* sized elements.

After modelling and meshing the acoustic model, the virtual model is adjusted to the physical test set up, by modifying the window mounting and the acoustic properties of the SAE interior according to the measurements of Müller [1].

Within the pre-processing of the vibro-acoustic simulation, the implementation of the window mounting is a major aspect, as the modal vibration behavior is considered to have a high impact on the perceptible sound spectrum in the vehicle. For validating the simulated vibration behavior, measurements of the SAE body are chosen as a validation basis for a simulative parameter study, leading to four different comparative eigenmodes

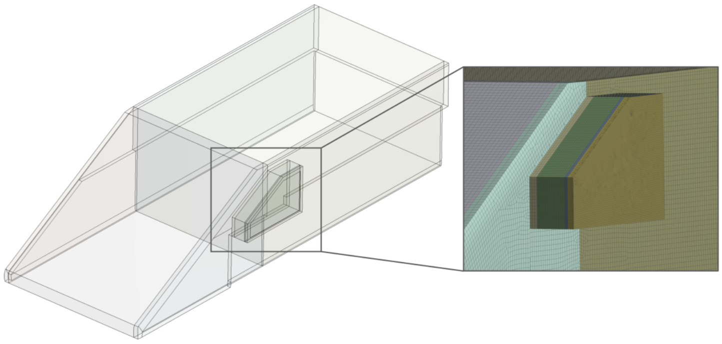

Figure 4: Geometry and mesh of the SAE body interior

at $f_m = 120\,Hz$, $f_m = 190\,Hz$, $f_m = 412\,Hz$ and $f_m = 705\,Hz$. To evaluate the accordance between measurements and simulation, the criteria *similar deformation pattern* and *matching natural frequency* are defined preliminary.

Figure 5: Abstraction of the mounting system for the simulative approach

In the virtual model, a complex modelling procedure is avoided by applying an elastic mounting system instead of modelling the entire mounting geometry (see fig. 5). Based on the equation for the elastic foundation stiffness (EFS), provided by Ansys [3] the elastic mounting is applied to a $10\,cm$ frame around the simplified window geometry. The EFS is then iteratively optimized, which yields the deformation patterns and the corresponding frequencies shown in picture 6.

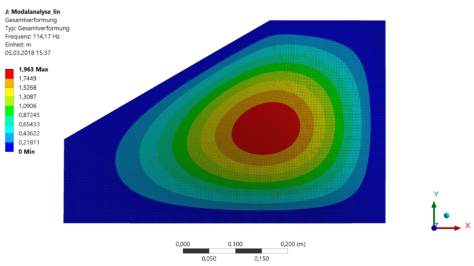

(i) $f_m = 114,17\,Hz$

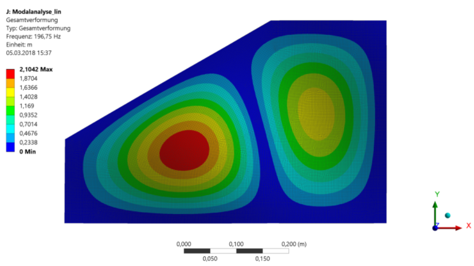

(ii) $f_m = 196,75\,Hz$

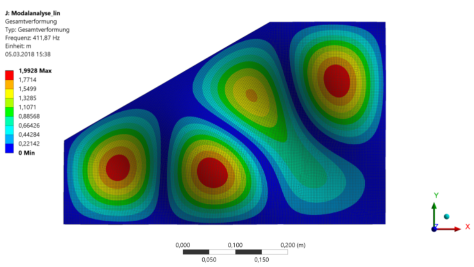

(iii) $f_m = 411,87\,Hz$

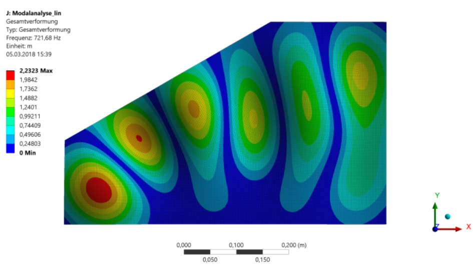

(iv) $f_m = 721,68\,Hz$

Figure 6: Eigenfrequencies for the comparative mode cases

The highest deviation of the simulated frequency occurs for the first modal frequency and yields an error of approximately 5%, which is acceptable. Also, the number and orientation of the deformed areas demonstrate an overall good accordance to the experiment. Only the highest comparative eigenmode shows a slight shift of the deformation areas to the upper window edges but is acceptable due to the necessary trade-off between the two criteria deformation pattern and frequency accuracy.

In the acoustic simulation domain, zero-displacement boundaries on all surfaces are added. Additionally, the damping characteristics of the individual wall paneling are transferred into the virtual model and implemented as absorption boundaries. To validate the resulting acoustic properties of the SAE-body interior, the reverberation time is calculated from the defined material properties according to the Sabine formulation [4] and then compared to measurements with the wind tunnel model [1]. Thereby the applied damping coefficients are adjusted for a better representation of the real model behavior.

3. ANALYSIS OF THE FLOW FIELD

The highly turbulent wake behind the side mirror geometry is a direct result of different turbulence mechanisms, which include a horse shoe vortex, the geometrical induced separation at the front edges of the mirror geometry and the overflow of the A- pillar. The interaction of these turbulence mechanisms, coupled with the aerodynamic drag of the blunt mirror body leads to the formation of a dead water immediately behind the mirror. Through the interaction of the fast, separated fluid with the slow fluid in the dead water area, a high level of turbulence occurs around the dead water, which further downstream develops into the turbulent wake of the mirror. The impact of the highly turbulent areas on the surface of the SAE body can be visualized by the distribution of the wall shear stress (see fig. 7).

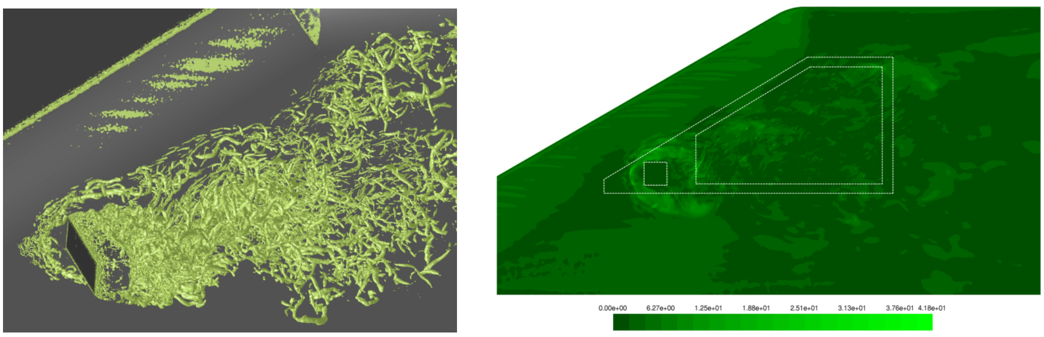

(i) ISO surface of the Q-criteria

(ii) Distribution of the wall shear stress, relative to the window location

Figure 7: Visualization of the turbulent structures near the window

Additionally, the distribution of turbulences in the wake is suppressed along the upper edge of the window, where fast fluid flows over the A-pillar and prevents the turbulent domain to spread upwards. Behind the dead water area, the finer distribution of the wall shear stress indicates an increase of small scaled turbulences and therefore a dissipation of the vortex structures.

The characteristic structure of the turbulent wake can be explained by the dynamics of the vortex structures surrounding the dead water. This vortex area changes size with a characteristic frequency, emitting vortices to the wake after reaching a maximum expansion. This process is well described in literature and known as pumping oscillation [5]. To capture this process in the simulative approach, six monitor planes are inserted in the turbulent wake of the mirror, to monitor the pressure development over the flow time. A Fast-Fourier-Transformation of the resulting time signals indicates a characteristic frequency of $55,55\,Hz$, which equals a time delta of $0,018\,s$ for one pumping cycle. A further analysis of the vortex distributions at four separate time steps inside this interval confirms the characteristic frequency as the pumping frequency. Furthermore, it is shown that in the process of emitting vortices downstream, the turbulences are concentrated alternating above and below the mirror center line. Thereby a structure similar to the Kármán vortex street is formed behind the mirror geometry. Considering the relative position of the window to the turbulent structures, it becomes clear, that only the upper structures are relevant for the excitation of the side window (see fig pic:wallsheerstress). Within the pre-processing of the captured pressure signals for the acoustic simulation, the time data is frequency transformed and exported from Ansys Fluent in the *cgns.* format (see fig. 8). Furthermore, this allows a frequency orientated treatment of the flow induced pressure fluctuations on the window surface (see fig 8).

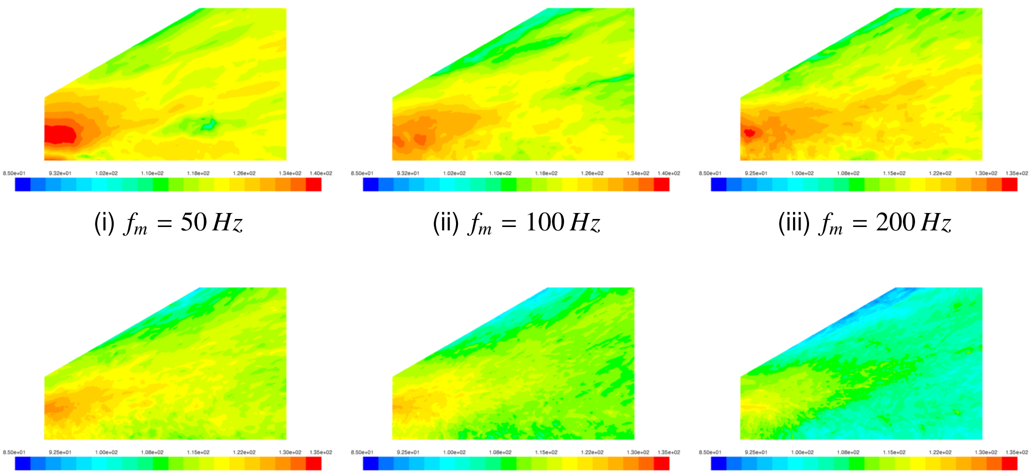

(i) $f_m = 50\,Hz$ (ii) $f_m = 100\,Hz$ (iii) $f_m = 200\,Hz$

(iv) $f_m = 500\,Hz$ (v) $f_m = 1000\,Hz$ (vi) $f_m = 2000\,Hz$

Figure 8: Third octave bands of the pressure distribution on the side window

The distribution of the frequency transformed pressure fluctuations in figure 8 indicates that the highest fluctuations occur in the vicinity of the mirror, while the magnitude of the pressure fluctuations declines with increasing distance to the mirror. The relatively low fluctuation amplitude along the upper window corner confirms the influence of the A-pillar overflow in the frequency domain. Also, the fluctuation magnitude becomes smaller for higher frequencies.

4. ACOUSTIC SIMULATION

The coupling of the fluid pressure to the vibro-acoustic simulation is implemented via *CFD Pressure Mapping* on the side window surface and a *Symmetric Algorithm* is used as solver option. The frequency range for the simulation is limited by the human hearing range $f_{min} = 20\,Hz$ and the approximated maximum frequency resolution of the flow simulation $f_{max} = 3000\,Hz$.

The accuracy of the simulation results is verified through the comparison to microphone measurements at the theoretical position of the driver's ear in the vehicle [1]. The microphone position is therefore transferred to the virtual model to capture the sound pressure at a similar location (see fig. 9).

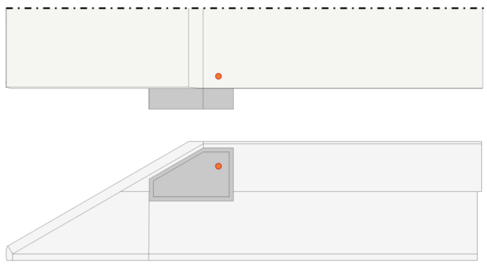

(i) Microphone position in the vehicle interior

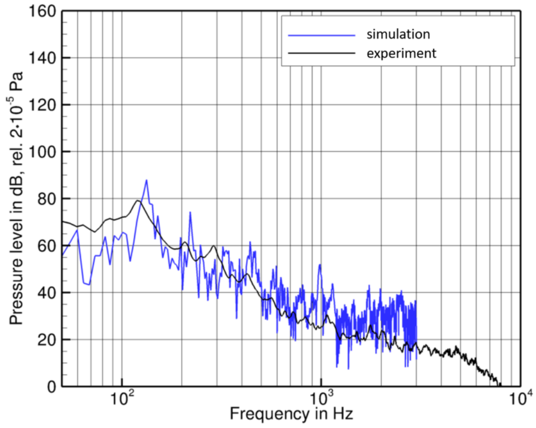

(ii) Measured and simulated sound pressure spectrum for comparison

Figure 9: Analysis of the simulation results

With a frequency resolution of $4,5\,Hz$, the simulation shows an overall good accordance to measurements below $2000\,Hz$ (see fig 9). Above this frequency, the sound pressure level of the measurements increasingly drops under the simulated curve.

This deviation of the sound pressure can be traced back to the maximum frequency resolution of the fluid simulation. Above $2000\,Hz$, the resolution of the fluid simulation isn't fine enough to resolve the entire spectrum of turbulent length scales, relevant for the excitement of the window. Consequently, the deviation occurs as a consequence of not fully resolving the dissipation of the vortices into smaller structures. As the dynamics of the vortex structures cause the window vibration, the deviation between measurements and simulation is a logical consequence of the too coarse resolution.

Focusing on the lower frequency areas, a slight deviation between the peaks in the measurement and the peaks in the simulation is apparent. For further investigations in this matter, an acoustic simulation with a non-absorbent vehicle interior is conducted and compared to the initial sound pressure spectrum (see fig. 10) .

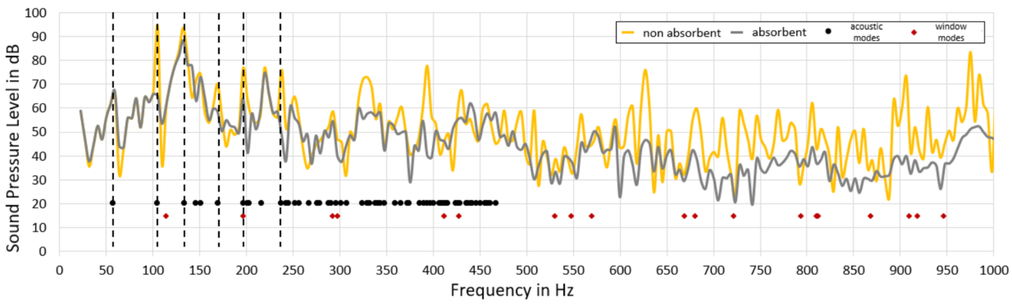

Figure 10: Comparison of the simulated sound spectra for absorbent and non-absorbent boundary conditions

Additionally, the first acoustic modes of the vehicle interior, shown in figure 11 and the natural frequencies of the window are taken into account.

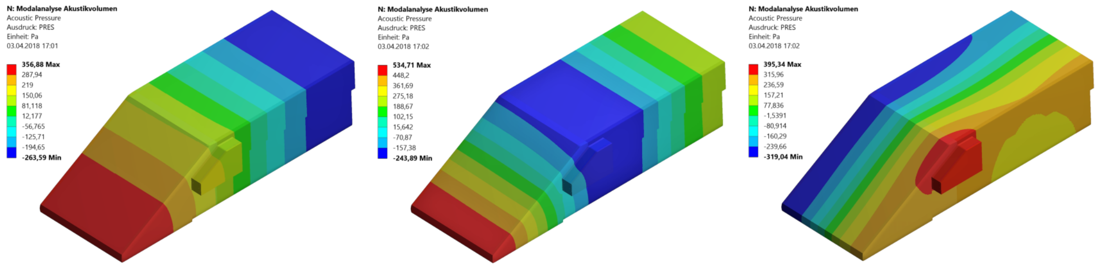

(i) $f_n = 57\,Hz$ (ii) $f_n = 105\,Hz$ (iii) $f_n = 134\,Hz$

Figure 11: First acoustic eigenmodes of the vehicle interior

The natural frequencies of the window and the acoustic volume are represented by discrete dots in the diagram. As displayed in figure 10, particularly in the low frequency domain, some peaks are damped, while others seem to be immune to the absorbing wall paneling inside the vehicle. To better understand this behavior three representative peaks are picked from the spectrum and analyzed in detail:

- **55 Hz**: According to the CFD simulation, this frequency represents the pumping frequency, where vortex structures are shed from the dead water area. For the present peak, the pumping frequency corresponds to the first natural frequency of the acoustic body, implying that the first acoustic resonance is excited by this characteristic turbulence mechanism, resulting in the non-dampable behavior visible.

- **105 Hz**: This peak in the frequency spectrum corresponds to the second natural frequency of the acoustic body, but is strongly damped, when simulated with absorbent boundary conditions. This leads to the assumption, that peaks in the spectrum, which are solely a result of the excitation of acoustic modes, can be damped by the application of absorption materials.

- **134 Hz**: The third peak of interest again corresponds to an acoustic eigenfrequency, but is barely damped in the absorbent simulation. Taking the natural frequencies of the window into account, the first window eigenfrequency can be found in the vicinity of this peak, at $f = 114\,Hz$. A peak, with a similar behavior is located at $f = 219\,Hz$, where also no damping is apparent and a natural frequency of the window is located nearby.

Assuming that window modes, excited by the pressure fluctuations cause non-dampable peaks in the simulated sound pressure spectrum, the probability of a shifted influence of the window modes in the resulting acoustic signal has to be taken into consideration.

As the simulated and the measured peaks in figure 11 show a similar offset, it is evident that this deviation can also be traced back to the shifted influence of the window eigenmodes. For a further investigation of this assumption, the acoustic simulation is repeated with a significantly higher mounting stiffness and therefore higher natural frequencies.

A comparison between the resulting spectrum and the initially simulated spectrum indicates, that the peaks at 134 Hz and 219 Hz were shifted to higher frequencies matching

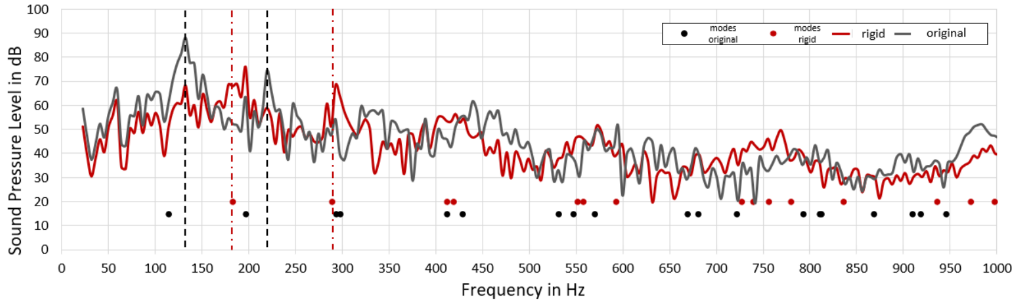

Figure 12: Influence of a higher mounting stiffness (rigid) on the spectrum of the sound pressure level

the shifting of the window modes (see fig. 12). This reinforces the previous assumption but does not yet provide a sufficient explanation for the deviation. The question however remains unanswered in the context of this paper and should be investigated by further research.

5. CONCLUSION

In this paper a numerical methodology for the simulation of a fluid-structure-acoustic interaction is presented. A SAE body with a simplified mirror geometry was chosen as test case, with the aim, to reproduce and to predict the perceptible sound spectrum inside the generic vehicle. As validation basis, reference measurements, conducted by Müller [1] were transferred to the test case.

For the flow simulation a DDES model was chosen in Ansys Fluent, while the vibro-acoustic simulation was performed separately in Ansys Mechanical. The transfer of the flow data to the vibroacoustic simulation was realized by exporting and importing the pressure fluctuations on the side window in the *cgns.* data format.

Furthermore, different boundary conditions, like absorption materials inside the vehicle interior, or the elastic fixation of the side window were implemented and adjusted to match the measured model characteristics. This enabled a targeted investigation of the individual influencing parameters. It could be shown that both elements have a high impact on the resulting sound pressure spectrum.

The simulated sound pressure spectrum shows an overall good accordance to the reference measurements, with two limitations. Firstly the deviation above 2000 Hz due to the maximum resolution of the fluid simulation and secondly the offset of characteristic peaks in the sound pressure spectrum. A first explanation for the offset was introduced and supported by first investigations but has not been clarified entirely.

6. REFERENCES

[1] Stefan Müller. *Fluid-Struktur-Akustik-Kopplung bei der Überströmung dünner Platten: Zugl.: Erlangen-Nürnberg, Univ., Diss., 2015*, volume 24 of *Schriftenreihe des Lehrstuhls für Prozessmaschinen und Anlagentechnik*. Shaker, Aachen, 2015.

[2] Ansys Inc. Tutorial: Simulation of aero-vibro-acoustic phenomena using ansys fluent and ansys mechanical: Test case: Noise inside a cavity with a vibrating wall, caused by the external turbulent flow.

[3] Sheldon Imaoka. Guideline: elastic foundation stiffness: Ansys technical support group.

[4] Peter Zeller. *Handbuch Fahrzeugakustik: Grundlagen, Auslegung, Berechnung, Versuch*. ATZ / MTZ-Fachbuch. Vieweg+Teubner Verlag, Wiesbaden, 2., überarbeitete auflage edition, 2012.

[5] Thomas Schütz, editor. *Hucho - Aerodynamik des Automobils: Strömungsmechanik, Wärmetechnik, Fahrdynamik, Komfort ; mit 49 Tabellen*. ATZ / MTZ-Fachbuch. Springer Vieweg, Wiesbaden, 6. , vollständig überarbeitete und erweiterte auflage edition, 2013.

[6] Mikhail S. Gritskevich, Andrey V. Garbaruk, Jochen Schütze, and Florian R. Menter. Development of ddes and iddes formulations for the k-w shear stress transport model. *Flow, Turbulence and Combustion*, 88(3):431–449, 2012.

[7] Marco Oswald. Aero-vibro-acoustics for wind noise application, 2015.